



Desferrioxamine-B adsorption to and iron dissolution from palygorskite and sepiolite

Mehran Shirvani*, Farshid Nourbakhsh

Department of Soil Science, College of Agriculture, Isfahan University of Technology, Isfahan, Iran

ARTICLE INFO

Article history:

Received 21 June 2009

Received in revised form 26 January 2010

Accepted 26 January 2010

Available online 2 February 2010

Keywords:

DFOB

Siderophore

Fibrous clays

Weathering

Kinetic

Isotherm

Fe

ABSTRACT

Dissolution weathering of minerals can be greatly affected by the presence of siderophores and their adsorption in soil environments. In this research, adsorption equilibria and kinetics of desferrioxamine-B (DFO-B) siderophore on palygorskite and sepiolite, minerals of arid and semiarid soils, were investigated. Iron (Fe) release pattern in the presence of increasing concentrations of DFO-B was also studied. Palygorskite represented a higher capacity but lower affinity for DFO-B adsorption compared to sepiolite. Retention of DFO-B by the minerals was initially rapid and then slowed down as time progressed. Time-dependent DFO-B adsorption to palygorskite and sepiolite was best described by the pseudo second-order and parabolic diffusion models, respectively. The presence of DFO-B enhanced the amount of Fe released from the clay minerals suggesting that siderophore-promoted dissolution might be one of the weathering mechanisms acting on these fibrous clay minerals. Iron concentrations measured in the equilibrium solutions with palygorskite and sepiolite were in the adequate Fe nutrition range for microorganisms and plant roots in soil environments.

© 2010 Elsevier B.V. All rights reserved.

1. Introduction

Iron is not a readily available nutrient for microorganisms and higher plants in neutral and alkaline environments. In response to low iron availability, microbial and plant-root cells synthesize and release some low-molecular-mass compounds, called siderophores. About 500 siderophores were identified, a great category of which possesses hydroxamic groups. Desferrioxamine-B (DFO-B) is a hexadentate hydroxamic siderophore secreted by bacteria and fungi in response to low iron availability. It binds Fe^{3+} with a stability constant near 10^{31} (Boukhalfa and Crumbliss, 2002).

As secreted into the environment, siderophores chelate Fe^{3+} which promotes dissolution of iron from minerals. Such ligand-controlled dissolution is proposed to be surface complex formation by ligand exchange reaction followed by detachment of the surface metal center and finally regeneration of the surface (Furrer and Stumm, 1986). Both the amount and the rate of iron dissolution from minerals are usually enhanced in the presence of siderophores (Kalinowski et al., 2000; Kraemer 2004). Watteau and Berthelin (1994) showed that Fe released from goethite in the presence of 126 μM DFO-B was twice as much as Fe mobilized from the same mineral by HCl solution at $\text{pH} = 3$. Buss et al. (2007) also observed extensive DFO-B-promoted pitting on an iron-silicate mineral demonstrating the potential role of this siderophore in chemical weathering of minerals in the environment. In several studies, dissolution enhancement of Al, Mn, and Si by DFO-B from various

minerals was also reported (Liermann et al., 2000; Duckworth and Sposito, 2007; Peña et al., 2007).

Adsorption on clay minerals could drastically affect the function of siderophores in soil environments. Since a portion of the siderophore may be irreversibly adsorbed to the soil particle surfaces, higher levels of a siderophore may be needed to saturate the clay surfaces and to provide sufficient siderophore for the iron release and nutrition of the cells (Lavie and Stotzky, 1986). Siderophores may be strongly adsorbed by clay minerals and lose their ability to detach and transfer iron into the solution. Siebner-Freibach et al. (2006) using FTIR and XRD analyses revealed adsorption mechanisms of DFO-B on montmorillonite as follows:

- 1- Hydrogen bonding between the N–H of the secondary amide groups of the siderophore and oxygen planes of the clay or adsorbed water molecules.
- 2- Bonding of hydroxamic C=O groups to the exchangeable cations through water bridges.
- 3- Hydrogen bonding of the hydroxamic O–H groups with the hydration water molecules of the exchangeable cations.
- 4- Adsorption of NH_3^+ groups indirectly via water molecules or directly to the oxygen planes of the clay minerals.

Palygorskite and, less commonly, sepiolite are fibrous clay minerals reported in soils of arid and semiarid regions (Galan, 1996; Khademi and Mermut, 1998). Investigating the interactions of siderophores with these minerals is vital to comprehend weathering reactions and iron acquisition efficiency of living cells in the soil environment. Little information is available about the adsorption of siderophores on palygorskite and

* Corresponding author. Fax: +98 311 3913471.

E-mail address: shirvani@cc.iut.ac.ir (M. Shirvani).

sepiolite. Our objectives were: 1) investigation of DFO-B adsorption equilibria and kinetics on palygorskite and sepiolite, 2) evaluation of the iron release pattern to show siderophore-promoted weathering of the fibrous clays as a potential process of supplying bioavailable Fe in the soil environment.

2. Materials and methods

2.1. Materials

Palygorskite of Florida (Source Clay Minerals Repository, Purdue University, IN) and sepiolite of Vicalvaro (TOLSA, Madrid, Spain) were used in this study. The samples were reacted with acetate buffer, hydrogen peroxide and citrate buffer to remove carbonates, organic matter and iron/manganese oxides impurities, according to the method of Kittrick and Hope (1963). The <2 μm fraction of the clay minerals were separated by centrifugation and saturated with Ca^{2+} using 0.5 M CaCl_2 solution. Excess salts were washed out until the electrical conductivity of eluents reached about $30 \mu\text{S m}^{-1}$. The Ca-clay minerals were freeze-dried. X-ray diffraction patterns obtained for orientated samples with a XD-610 Shimadzu X-Ray Diffractometer (Cu- α) indicated that the samples mainly contained palygorskite or sepiolite. The cation exchange capacity of Ca^{2+} -saturated palygorskite and sepiolite was 19.5 and 11 cmol kg^{-1} , determined by the ammonium acetate method (Rhoads, 1986). Specific surface areas of 136 and $240 \text{ m}^2 \text{ g}^{-1}$ were measured for palygorskite and sepiolite, using the BET- N_2 analysis.

Stock suspensions of the minerals (30 g L^{-1}) in 0.01 M CaCl_2 solution were prepared and kept at room temperature for 24 to 48 h until their pH reached to the constant values of 8.1 (palygorskite) and 8.7 (sepiolite).

Desferrioxamine mesylate $\text{C}_{25}\text{H}_{48}\text{N}_6\text{O}_8 \cdot \text{CH}_4\text{O}_3\text{S}$ (Sigma-Aldrich, USA) was used in this study as the source of DFO-B. This siderophore was chosen because it is commercially available and a reasonable research background about it was found in the literature (Kraemer, 2004). The schematic molecular structure of DFO-B is shown in Fig. 1.

2.2. Adsorption equilibrium experiments

Batch experiments were used for determination of DFO-B adsorption isotherms. Ten milliliter samples of the stock suspensions were pipetted into 50 mL centrifuge tubes and solutions containing eight different DFO-B concentrations were added to the samples. The initial siderophore concentrations were 0, 0.131, 0.163, 0.240, 0.407, 0.750, 0.927 and 1.831 mM and the adsorbent/solution ratio was 1/100. The ionic strength of the systems was fixed at 0.03 M with 0.01 M calcium chloride. A control sample (with no adsorbent) was also included for each DFO-B concentration level. The samples were then shaken on an

orbital shaker (160 rpm) for 24 h at $25 \pm 1 \text{ }^\circ\text{C}$. The equilibrium solutions were separated by centrifugation at 5000 g for 15 min. The concentration of iron released from the minerals was measured in the supernatant using an AAnalyst 200 Perkin-Elmer Atomic Absorption Spectrophotometer.

The concentration of DFO-B in the equilibrium solutions was determined colorimetrically by a Genway Spectrophotometer at 470 nm in the presence of excess iron salt according to the method described by Kraemer et al. (1999). To prevent precipitation of Fe (hydr)oxide, the pH value was adjusted at 2 by adding a predetermined volume of hydrochloric acid. After acidification, FeCl_3 was added to a final concentration of $312 \mu\text{M}$. Standards were prepared with siderophore concentrations of 0.017 to $0.258 \mu\text{M}$ and treated analogously to experimental samples. The amount of adsorbed DFO-B in each sample was calculated from the difference between initial and final concentrations in equilibrium solutions. The adsorbed DFO-B values were then plotted against the corresponding equilibrium concentrations and two familiar models, Langmuir and Freundlich, were tested to describe the adsorption behavior.

Determination coefficients (r^2) and standard errors of estimate (SEE) were calculated and compared to evaluate goodness of fit of the models. The SEE values were calculated from:

$$SEE = \left[\frac{\sum (q_e - q'_e)^2}{n-2} \right]^{1/2} \quad (1)$$

where, q_e and q'_e are measured and model estimated DFO-B adsorbed on each clay minerals at equilibrium, respectively, and 'n' is the number of measurements.

2.3. Adsorption kinetic experiments

The rates of DFO-B retention by palygorskite and sepiolite were also evaluated using batch experiments. Adsorption tests were started by simultaneously adding 100 mL of 3.5 mM DFO-B to 200 mL of the mineral suspension, agitated vigorously by a magnetic stirrer in a 500 mL glass reaction vessel at $25 \pm 1 \text{ }^\circ\text{C}$. The concentration of DFO-B at the beginning of the experiment was 1 mM and the mineral/solution ratio was 1/100. Duplicate samples (each one 10 mL) were pipetted out at ten selected time intervals (from 10 to 1440 min), centrifuged and analyzed for the residual DFO-B concentration in solutions. The concentrations of DFO-B in the supernatants were determined as described in Section 2.2. The amount of DFO-B adsorbed on the minerals at each time was calculated from the difference between the initially added and finally measured DFO-B concentrations. The time-dependent adsorption data were then tested to be described by various kinetic models.

2.4. Curve fitting and data analysis

Curve fitting using non-linear regression analysis and graph preparations were carried out with the statistical package GraphPad Prism (version 4.00 for Windows, GraphPad Software, San Diego, California, USA).

3. Results and discussion

3.1. Equilibrium DFO-B adsorption

Desferrioxamine-B adsorption data on the fibrous clay minerals were well described by both the Langmuir and Freundlich models. Fitted isotherm parameters and their corresponding coefficient of determinations and standard errors are shown in Table 1. The Langmuir equation provided slightly better correlations for DFO-B adsorption on palygorskite, while adsorption of the siderophore on

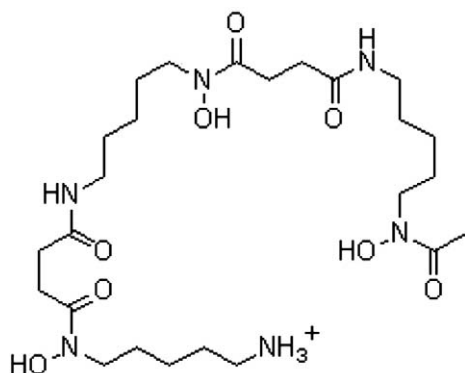


Fig. 1. Molecular structure of desferrioxamine-B.

Table 1

Fitted isothermal parameters of DFO-B adsorption on palygorskite and sepiolite minerals.^a

| Isotherm | Parameter | Palygorskite | Sepiolite | |
|------------|--|---------------------------|-----------|-------|
| Langmuir | r^2 | 0.977 | 0.948 | |
| | $q_i = \frac{q_{\max} K_L C_i}{1 + K_L C_i}$ | SEE ($\mu\text{mol/g}$) | 1.435 | 2.356 |
| | q_{\max} ($\mu\text{mol/g}$) | 46.50 | 41.56 | |
| | K_L ($\text{L}/\mu\text{mol}$) | 0.875 | 1.909 | |
| Freundlich | r^2 | 0.972 | 0.983 | |
| | $q_i = K_F C_i^{1/n}$ | SEE ($\mu\text{mol/g}$) | 1.590 | 1.353 |
| | K_F ($\mu\text{mol}^{(1-1/n)} \text{g}^{-1} \text{L}^{1/n}$) | 20.81 | 26.45 | |
| | $1/n$ | 0.639 | 0.499 | |

^a q_i is the amount of DFO-B adsorbed at equilibrium; C_i the equilibrium DFO-B concentration; q_{\max} the maximum adsorption capacity; K_L an affinity parameter; K_F and n are constants; r^2 the determination coefficient; SEE standard error of estimate; all r^2 values are significant at the 0.001 probability level.

sepiolite was relatively better described by the Freundlich model (Table 1).

Adsorption of DFO-B on montmorillonite (Siebner-Freibach et al., 2004) and deoxymugineic acid on goethite (Reichard et al., 2005) was also satisfactorily modeled by the Langmuir equation. Desferrioxamine-B adsorption maxima estimated by the Langmuir equation (q_{\max}) were 46.5 and 41.6 $\mu\text{mol g}^{-1}$ for palygorskite and sepiolite, respectively. Considering of DFO-B molecular cross-sectional area of 1.65 nm² (Haak et al., 2003), it can be calculated that only about 34 and 17% of the specific N₂-BET surface area of palygorskite and sepiolite covered by DFO-B molecules, at the highest DFO-B concentration applied. It seems that DFO-B was mainly adsorbed on the external clay mineral surfaces and hardly able to enter the structural channels of the palygorskite and sepiolite with dimensions of 0.37 × 0.60 and 0.56 × 1.10 nm. Neubauer et al. (2002) reported that the DFO-B adsorption maximum of ferrihydrite reached about 30 $\mu\text{mol g}^{-1}$ after 7–8 days of equilibration with 70 μM DFO-B.

The adsorption capacities of the fibrous clay minerals for DFO-B were much higher than 1.5 and 5.15 $\mu\text{mol g}^{-1}$ reported by Kraemer et al. (1999) and Rosenberg and Maurice (2003) for goethite and kaolinite, respectively. Cheah et al. (2003) related low DFO-B adsorption capacity of goethite (1.2 $\mu\text{mol g}^{-1}$) to repulsion of DFO-B cations by the positively charged goethite surface and to steric hindrance while DFO-B molecules bind Fe centers in the mineral surfaces. For montmorillonite, DFO-B adsorption maxima as high as 480 and 550 $\mu\text{mol g}^{-1}$ were calculated by Haack et al. (2008) and Siebner-Freibach et al. (2004). The negative charges of the clay mineral layers and the penetration of DFO-B molecules into the interlayer spaces were the causes of such high adsorption of DFO-B siderophore by montmorillonite (Siebner-Freibach et al., 2004, 2006; Haack et al., 2008).

The Langmuir affinity parameter (K_L) was 0.875 and 1.909 L g^{-1} for palygorskite and sepiolite, indicating that DFO-B adsorbs on sepiolite much stronger than on palygorskite.

3.2. Iron release

The amount of iron released from palygorskite and sepiolite increased nonlinearly and reached about 6.15 and 2.7 $\mu\text{mol g}^{-1}$ with increasing the initial DFO-B concentration from 0.13 to 1.8 mM (Fig. 2). In contrast to palygorskite, iron release from sepiolite reached a constant value of ~2.7 $\mu\text{mol g}^{-1}$ at about 0.6 mM of DFO-B (Fig. 2). This may confirm that fewer amounts of releasable Fe ions existed on the sepiolite surfaces was the limiting factor of iron dissolution from this mineral. In fact, Vicalvaro sepiolite is a magnesium-rich silicate with only 0.56 Fe₂O₃% (Santaren et al., 1990) whereas Florida palygorskite contains 3.74% Fe₂O₃ (Mermut and Cano, 2001).

Soluble iron in the equilibrium solutions showed a nonlinear relationship with the equilibrium DFO-B concentration (Fig. 3), confirming the role of the siderophore in chemical weathering and Fe dissolution from the fibrous clay minerals. Even in the presence of

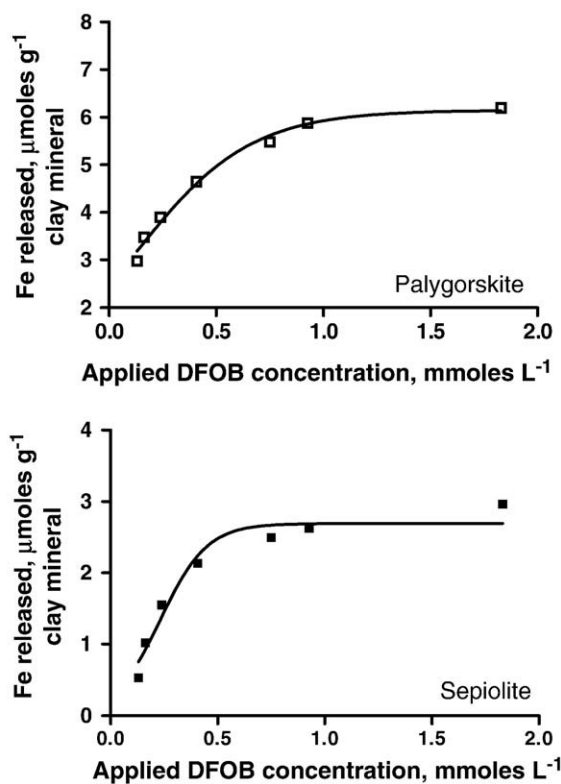


Fig. 2. Relationship between applied initial concentration of DFO-B and iron release.

DFO-B concentrations <200 μM , the dissolved Fe concentration in the clay mineral suspensions was considerable (at least 0.5 $\mu\text{mol L}^{-1}$). It suggests that these fibrous minerals possess a significant potential of furnishing iron to the living cells in the soil environments. Rosenberg

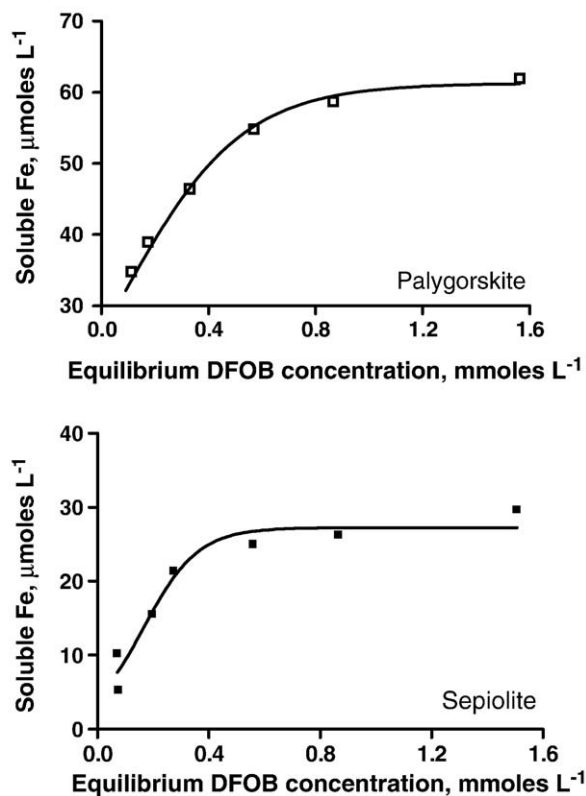


Fig. 3. Relationship between equilibrium concentration of DFO-B and soluble iron.

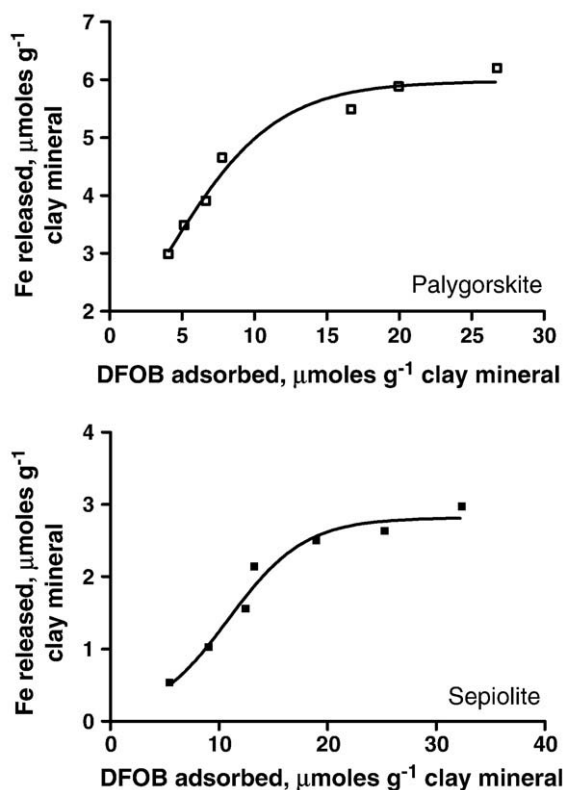


Fig. 4. Relationship between amounts of DFO-B adsorbed and iron released.

and Maurice (2003) reported that Fe released from kaolinite in the presence of 240 μM DFO-B over 96 h at pH 5.5 was only $0.2 \mu\text{mol L}^{-1}$ (~ 10 ppb). Based on microbial growth experiments, Maurice et al. (2001) and Ams et al. (2002), stated that such a low Fe level ($0.2 \mu\text{mol L}^{-1}$) was sufficient for metabolic requirements of aerobic microorganisms. At very high DFO-B concentrations (i.e. 1.6 mM), iron concentrations up to about 60 and 30 μM were generated by the dissolution of palygorskite and sepiolite. Neubauer et al. (2002) also observed an Fe concentration as high as 80 μM released from ferrihydrite after 4 days of interacting with 100 μM DFO-B.

Significant correlations were found between the released Fe and adsorbed DFO-B in the clay mineral suspensions (Fig. 4). This may imply that a ligand-promoted surface-controlled dissolution mechanism occurred during iron release from the palygorskite and sepiolite. A similar conclusion was drawn by Rosenberg and Maurice (2003) studying DFO-B adsorption on kaolinite.

3.3. Desferrioxamine-B adsorption kinetics

Desferrioxamine-B adsorption on palygorskite and sepiolite were initially rapid and pseudo equilibrium conditions were reached within about 24 h. Haack et al. (2008) showed that DFO-B adsorption equilibration time on montmorillonite is considerably variable depending on the type of the saturating cation. They reported that DFO-B adsorption rapidly reached a steady-state condition within 1 h with Na- and Mg-montmorillonite but in 24 h to K-smectite. Siebner-Freibach et al. (2004) also reported that most of the DFO-B adsorption on Ca-montmorillonite took place within the first hour. Adsorption equilibration times and rate values reported in the literature, however, should be critically considered, because adsorption of siderophores on colloidal soil particles is greatly dependent on sorbent characteristics, solution chemistry, and environmental factors.

The pseudo second-order model best fitted the DFO-B adsorption on palygorskite (Table 2). If the experimental data follows a pseudo second-order equation, the sorption process may be described as

Table 2
Desferrioxamine-B adsorption kinetic parameters on palygorskite and sepiolite minerals.*

| Equation | Parameter | Palygorskite | Sepiolite |
|---|--|---------------------|---------------------|
| Pseudo first-order: $Q_t = Q_{e1}(1 - e^{-k_1 Q_{e1} t})$ | Q_{e1} ($\mu\text{mol g}^{-1}$) | 77.86 | 87.81 |
| | $k_1 \times 10^3$ (min^{-1}) | 4.73 | 4.84 |
| | r^2 | 0.768** | 0.115 ^{ns} |
| Pseudo second-order: $Q_t = \frac{k_2 Q_{e2}^2 t}{1 + k_2 Q_{e2} t}$ | Q_{e2} ($\mu\text{mol g}^{-1}$) | 78.16 | 88.81 |
| | $k_2 \times 10^2$ ($\text{g } \mu\text{mol}^{-1} \text{min}^{-1}$) | 4.52 | 4.21 |
| | r^2 | 0.911*** | 0.390 ^{ns} |
| Elovich: $Q_t = a + b \ln t$ | SEE ($\mu\text{mol g}^{-1}$) | 0.235 | 1.002 |
| | a | 75.93 | 84.34 |
| | b | 0.36 | 0.71 |
| Power function: $Q_t = mt^n$ | r^2 | 0.598* | 0.858*** |
| | SEE ($\mu\text{mol g}^{-1}$) | 0.498 | 0.484 |
| | m | 75.96 | 84.38 |
| Parabolic diffusion: $Q_t = C + Rt^{1/2}$ | $n \times 10^3$ | 4.67 | 8.15 |
| | r^2 | 0.596* | 0.861*** |
| | SEE ($\mu\text{mol g}^{-1}$) | 0.500 | 0.479 |
| Parabolic diffusion: $Q_t = C + Rt^{1/2}$ | C | 77.10 | 86.16 |
| | $R \times 10^2$ | 4.04 | 11.22 |
| | r^2 | 0.315 ^{ns} | 0.910*** |
| | SEE ($\mu\text{mol g}^{-1}$) | 0.651 | 0.385 |

* Q_t is the amount of DFO-B adsorbed at time t ; Q_{e1} and Q_{e2} are the model estimated amounts of DFO-B adsorbed at equilibrium, respectively; k_1 and k_2 are apparent first- and second-order rate constants, respectively; a , b , m , n , R and C are constants; r^2 is the determination coefficient; SEE is the standard error of estimate; ns, *, ** and *** are nonsignificant and significant at the 0.05, 0.01 and 0.001 probability levels, respectively.

chemisorptions (Ho et al., 1995). Regarding adsorption of DFO-B on sepiolite, the parabolic diffusion equation described the data better than did the other equations, indicating that diffusion controlled phenomena may be rate-limiting (Sparks, 2003). The Power and Elovich equations also adequately described the DFO-B adsorption kinetics on sepiolite, but these two models had lower r^2 and higher SEE values compared to the parabolic diffusion equation. Parravano and Boudart (1955) noted that a number of different processes, including bulk and surface diffusion as well as chemisorption, might be described by the Elovich equation. Hence, one can conclude that adsorption of DFO-B to sepiolite might proceed by both diffusion- and surface-controlled reactions.

4. Conclusions

Palygorskite and sepiolite had considerable capacity to adsorb the DFO-B siderophore. The adsorption was satisfactorily modeled by the Langmuir and Freundlich isotherms. Adsorption rates of DFO-B and equilibration time varied from the palygorskite to the sepiolite. This may be related to the structural and compositional differences of the two clay minerals. Further spectroscopic researches are needed to improve our understanding of the mechanisms involved in DFO-B interaction with palygorskite and sepiolite. Iron release from the palygorskite and sepiolite was enhanced in the presence of DFO-B. The siderophore, therefore, can promote dissolution (weathering) of palygorskite and sepiolite in the soil environment.

References

- Ams, D.A., Maurice, P.A., Hersman, L.E., Forsythe, J.H., 2002. Siderophore production by an aerobic *Pseudomonas mendocina* bacterium in the presence of kaolinite. Chem. Geol. 188, 161–170.
- Boukhalfa, H., Crumbliss, A.L., 2002. Chemical aspects of siderophore mediated iron transport. BioMetals 15, 325–339.
- Buss, H.L., Lüttge, A., Brantley, S.L., 2007. Etch pit formation on iron silicate surfaces during siderophore-promoted dissolution. Chem. Geol. 240, 326–342.
- Cheah, S.F., Kraemer, S.M., Cervini-Silva, J., Sposito, G., 2003. Steady-state dissolution kinetics of goethite in the presence of desferrioxamine B and oxalate ligands: implications for the microbial acquisition of iron. Chem. Geol. 198, 63–75.
- Duckworth, O.W., Sposito, G., 2007. Siderophore-promoted dissolution of synthetic and biogenic layer-type Mn oxides. Chem. Geol. 242, 497–508.

- Furrer, G., Stumm, W., 1986. The coordination chemistry of weathering. 1. Dissolution kinetics of δ -Al₂O₃ and BeO. *Geochim. Cosmochim. Acta* 50, 1847–1860.
- Galan, E., 1996. Properties and applications of palygorskite–sepiolite clays. *Clay Miner.* 31, 443–453.
- Haack, E.A., Johnston, C.T., Maurice, P.A., 2008. Mechanisms of siderophore sorption to smectite and siderophore-enhanced release of structural Fe³⁺. *Geochim. Cosmochim. Acta* 72, 3381–3397.
- Ho, Y.S., Wase, D.A.J., Forster, C.F., 1995. Batch nickel removal from aqueous solution by sphagnum moss peat. *Water Res.* 29, 1327–1332.
- Kalinowski, B.E., Liermann, L.J., Givens, S., Brantley, S.L., 2000. Rates of bacteria-promoted solubilization of Fe from minerals: a review of problems and approaches. *Chem. Geol.* 169, 357–370.
- Khademi, H., Mermut, A.R., 1998. Submicroscopy and stable isotope geochemistry of carbonates and associated palygorskite in selected Iranian Aridisols. *Eur. J. Soil Sci.* 50, 207–216.
- Kittrick, J.A., Hope, E.W., 1963. A procedure for the particle size separation of soils for X-ray diffraction analysis. *Soil Sci.* 96, 312–325.
- Kraemer, S.M., 2004. Iron oxide dissolution and solubility in the presence of siderophores. *Aqua. Sci.* 66, 3–18.
- Kraemer, S.M., Cheah, S.F., Zapf, R., Xu, J., Raymond, K.N., Sposito, G., 1999. Effect of hydroxamate siderophores on Fe release and Pb(II) adsorption by goethite. *Geochim. Cosmochim. Acta* 63, 3003–3008.
- Lavie, S., Stotzky, G., 1986. Interactions between clay minerals and siderophores affect the respiration of *histoplasma capsulatum*. *Appl. Environ. Microbiol.* 51, 74–79.
- Liermann, L.J., Kalinowski, B.E., Brantley, S.L., Ferry, J.G., 2000. Role of bacterial siderophores in dissolution of hornblende. *Geochim. Cosmochim. Acta* 64, 587–602.
- Maurice, P.A., Vierkorn, M.A., Hersman, L.E., Fulghum, J.E., 2001. Dissolution of well and poorly ordered kaolinites by an aerobic bacterium. *Chem. Geol.* 180, 81–97.
- Mermut, A.R., Cano, A.F., 2001. Baseline studies of the Clay Minerals Society source clays: chemical analyses of major elements. *Clay. Clay Miner.* 49, 381–386.
- Neubauer, U., Furrer, B.G., Schulin, R., 2002. Heavy metal sorption on soil minerals affected by the siderophore desferrioxamine B: the role of Fe(III)(hydr)oxides and dissolved Fe(III). *Eur. J. Soil Sci.* 53, 45–55.
- Parravano, G., Boudart, M., 1955. In: Komarewsky, W.G., Rideal, V.I., Frankenburg, E.K. (Eds.), *Advances in Catalysis*. Academic Press, New York, pp. 47–74.
- Peña, J., Duckworth, O.W., Bargar, J.R., Sposito, G., 2007. Dissolution of hausmannite (Mn₃O₄) in the presence of the trihydroxamate siderophore desferrioxamine. *Geochim. Cosmochim. Acta* 71, 5661–5671.
- Reichard, P.U., Kraemer, S.M., Frazier, S.W., Kretzschmar, R., 2005. Goethite dissolution in the presence of phytosiderophores: rates, mechanisms, and the synergistic effect of oxalate. *Plant Soil* 276, 115–132.
- Rhoads, J.W., 1986. Cation exchange capacity. In: Page, C.A. (Ed.), *Methods of Soil Analysis, Part 2*, ASA, Madison, WI, pp. 149–158.
- Rosenberg, D.R., Maurice, P.A., 2003. Siderophore adsorption to and dissolution of kaolinite at pH 3 to 7 and 22 °C. *Geochim. Cosmochim. Acta* 67, 223–229.
- Santaren, J., Sanz, J., Ruiz-Hitzky, E., 1990. Structural fluorine in sepiolite. *Clay. Clay Miner.* 38, 63–68.
- Siebner-Freibach, H., Hadar, Y., Chen, Y., 2004. Interaction of iron chelating agents with clay minerals. *Soil Sci. Soc. Am. J.* 68, 470–480.
- Siebner-Freibach, H., Hadar, Y., Yariv, S., Lapidés, I., Chen, Y., 2006. Thermospectroscopic study of the adsorption mechanism of the hydroxamic siderophore ferrioxamine B by calcium montmorillonite. *J. Agri. Food Chem.* 54, 1399–1408.
- Sparks, D.L., 2003. *Environmental Soil Chemistry*, 2nd edition. Academic Press, New York.
- Watteau, F., Berthelin, J., 1994. Microbial dissolution of iron and aluminum from soil minerals—efficiency and specificity of hydroxamate siderophores compared to aliphatic-acids. *Eur. J. Soil Biol.* 30, 1–9.